PHYSICAL REVIEW B **91**, 041405(R) (2015)

Highly unconventional surface reconstruction of Na_2IrO_3 with persistent energy gap

F. Lüpke,[1,2] S. Manni,[3,4] S. C. Erwin,[5] I. I. Mazin,[5] P. Gegenwart,[4] and M. Wenderoth[1,*]

[1]*IV. Physikalisches Institut, Georg-August-Universität Göttingen, D-37077 Göttingen, Germany*

[2]*Peter Grünberg Institut (PGI-3), Forschungszentrum Jülich, D-52425 Jülich, Germany*

[3]*I. Physikalisches Institut, Georg-August-Universität Göttingen, D-37077 Göttingen, Germany*

[4]*Experimental Physics VI, Center for Electronic Correlations and Magnetism, University of Augsburg, D-86159 Augsburg, Germany*

[5]*Center for Computational Materials Science, Naval Research Laboratory, Washington, DC 20375, USA*

(Received 18 July 2014; published 12 January 2015)

Na_2IrO_3 is an intriguing material for which spin-orbit coupling plays a key role. Theoretical predictions have been made that the surface of Na_2IrO_3 should exhibit a clear signature of the quantum spin Hall effect. We studied the surface of Na_2IrO_3 using scanning tunneling microscopy and density-functional theory calculations. We observed atomic level resolution of the surface and two types of terminations with different surface periodicity and Na content. By comparing bias-dependent experimental topographic images to simulated images, we determined the detailed atomistic structure of both observed surfaces. One of these reveals a strong relaxation to the surface of Na atoms from the subsurface region two atomic layers below. Such dramatic structural changes well below the surface are highly unusual and cast doubt on any prediction of surface properties based on bulk electronic structure. Indeed, using spatially resolved tunneling spectroscopy, we found no indication of the predicted quantum spin Hall behavior.

DOI: 10.1103/PhysRevB.91.041405 PACS number(s): 68.35.B−, 68.37.Hk, 71.15.Mb, 73.20.−r

Novel states with unusual topological and frustrated properties have recently been predicted to arise in heavy transition-metal oxides, such as iridates, from a combination of interactions—spin-orbit coupling, Coulomb correlations, Hund's rule coupling, and one-electron hopping—with comparable energy scales [1–7]. Na_2IrO_3 is a prototypical material in the iridate family. It consists of an alternating stacking of honeycomb Ir_2NaO_6 layers separated by hexagonal Na_3 layers [8]. While many works have concentrated on unusual magnetic properties of the bulk material, the surface of Na_2IrO_3 may also reveal unusual physics. For example, recent work predicts quantum spin Hall (QSH) behavior in Na_2IrO_3 [2]. The resulting band topology should lead to helical edge states at the surface, which would be manifested experimentally by the closing of the band gap [2].

The prediction of QSH behavior was based on a tight-binding model derived from the bulk electronic structure [2]. It was subsequently shown that the bulk states depend very sensitively on the assumed geometry—in particular, on the positions of Na and rotations of the IrO_6 octahedra [7]. An important question is whether the geometry at the surface of Na_2IrO_3 is sufficiently similar to the bulk to support the assumptions underlying the QSH prediction. In this Rapid Communication, we used scanning tunneling microscopy (STM) and spectroscopy (STS) together with density-functional theory (DFT) calculations to address this question. We also tested the QSH prediction directly by spectroscopically probing for gap closure on the surface. Our most important findings are that (1) the surface of Na_2IrO_3 strongly reconstructs in a highly unconventional manner, which very likely undermines the conditions for QSH behavior, and (2) the surface gap does *not* close, which establishes that QSH behavior is indeed not realized at the Na_2IrO_3 surface.

Na_2IrO_3 surfaces were prepared *in situ* by cleaving parallel to the IrO honeycomb layers and at a base pressure of $p < 10^{-10}$ mbar at 300 K. After transfer to a home-built STM operating at 80 K within a few minutes and subsequent thermalization over a few hours, the surface was investigated by STM and STS to map occupied and unoccupied states and simultaneously access spatial variations of surface properties by recording $I(V)$ curves at every scan point. On the freshly cleaved surface, two different stable surface terminations were found in constant-current topographic measurements, both showing atomic level resolution (Fig. 1). The periodicity of the terminated surfaces suggests cleaving along the *ab* plane of the crystal. One termination shows the periodicity of bulk Na_2IrO_3 and is labeled as 1×1 in the following. The second termination shows a $(\sqrt{3} \times \sqrt{3})R30^\circ$ reconstruction. We have observed both terminations in roughly the same proportion in STM, however, the macroscopic ratio needs to be determined by further experiments. While the 1×1 surface shows a long-range periodic structure over tens of nanometers, the $(\sqrt{3} \times \sqrt{3})R30^\circ$ surface exhibits many defects and is well ordered only on the scale of a few nanometers. Note that in STM measurement at 300 K we observed the same 1×1 periodicity in the empty states and insulating behavior on this surface. However, the unstable tunneling conditions did not allow us to observe any filled states images or the $(\sqrt{3} \times \sqrt{3})R30^\circ$ surface.

Cleaving almost certainly leaves the strongly bonded IrO_6 octahedra intact while the Na is expected to be volatile. Hence, the observation of two different surface terminations suggests that cleaving creates two surfaces of similar stability with different Na coverage and hence different periodicity. We used DFT to determine the equilibrium geometries of different candidate surfaces with varying Na content in the top layer as well as subsurface layers. Total energies and forces were calculated within the Perdew-Burke-Ernzerhof (PBE) generalized-gradient approximation using projector augmented-wave potentials, as implemented in VASP [9,10].

*Corresponding author: mwender@gwdg.de

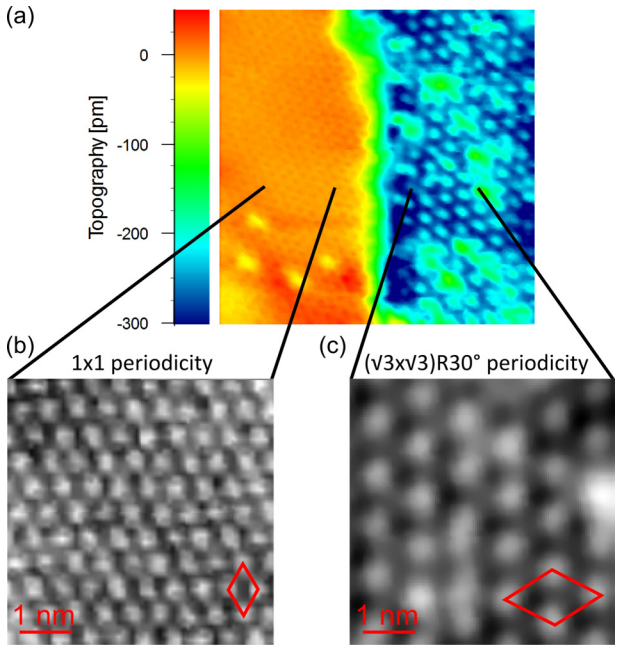

FIG. 1. (Color online) Constant-current STM topographic images at sample bias $V_{\text{bias}} = +2$ V. (a) Two different surface configurations with domain boundaries of few nm in lateral dimension are observed. (b) Detail of the 1×1 surface and (c) $(\sqrt{3} \times \sqrt{3})R30^\circ$ surface, with the respective unit cells indicated. The 1×1 surface exhibits long-range order, while the $(\sqrt{3} \times \sqrt{3})R30^\circ$ surface exhibits many defects and only local order.

After relaxation, we simulated STM images using the method of Tersoff and Hamann [11], by integrating the local density of states (LDOS) from -2 to 0 eV for the filled states and 0 to $+2$ eV for the empty states. The surface of constant integrated LDOS then corresponds to the ideal STM topography at that bias voltage.

Figure 2 shows the theoretical equilibrium structure and STM imagery for the two models that best reproduce the imagery of the two observed surfaces. The 1×1 surface shown in Fig. 2(a) was constructed by starting from the bulk crystal, which consists of stacked atomic layers in the stoichiometric sequence $\cdots|\text{Na}_3|\text{O}_3|\text{Na}_1,\text{Ir}_2|\text{O}_3|\cdots$. By cleaving this crystal within the pure Na layer, one obtains surfaces with different relative Na content. For reference, the ideal stoichiometric surface has a $\text{Na}_{3/2}$ surface layer. We constructed the 1×1 surface in Fig. 2(a) by removing one-third of the Na atoms from this idealized surface. Hence the model in Fig. 2(a) is $\text{Na}_1|\text{O}_3|\text{Na}_1,\text{Ir}_2|\text{O}_3|\cdots$. The agreement between simulated and measured constant-current topographies is excellent, strongly suggesting that this structural model is correct. In particular, the strong contrast inversion between empty and filled states observed experimentally is well reproduced in the simulated images. Even the detailed topography agrees well: The filled states appear as a bright honeycomb network, while the empty states appear as disconnected bright spots. The contrast reversal arises from different tunneling paths for positive and negative biases, via empty Na states and filled O states, respectively.

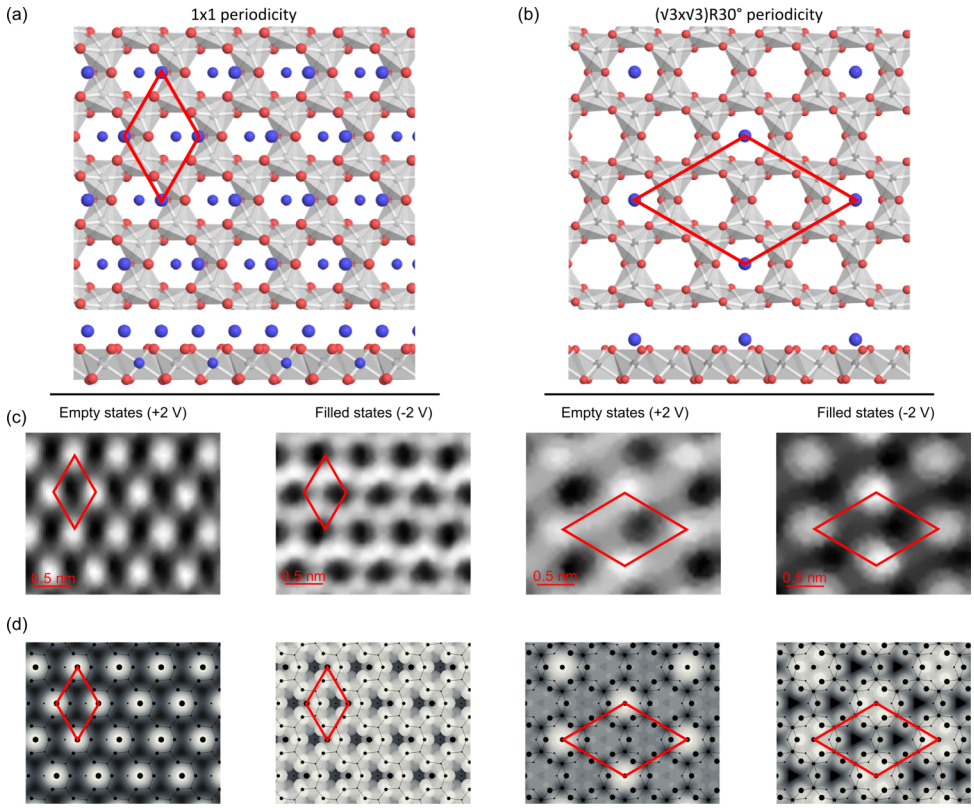

FIG. 2. (Color online) (a), (b) Theoretically determined structural models for 1×1 and $(\sqrt{3} \times \sqrt{3})R30^\circ$ surfaces viewed from the top and side, respectively (Na: blue; Ir: gray; O: red). Na atoms in the topmost layer are shown larger for clarity. (c) Experimental and (d) theoretically simulated STM images at $V_{\text{bias}} = \pm 2$ V. On the 1×1 surface, there is a clear contrast reversal between empty and filled states. On the $(\sqrt{3} \times \sqrt{3})R30^\circ$ surface, the dominant bright features for empty and filled images are located at the same positions.

Figure 2(b) shows an even more substoichiometric surface created by removing the entire topmost Na layer as well as two-thirds of the Na atoms in the subsurface Ir-Na layer. The nominal structure of this surface is hence $O_3|Na_{1/3},Ir_2|O_3|\cdots$, which indeed has the experimentally observed $(\sqrt{3}\times\sqrt{3})R30^\circ$ periodicity [12]. Upon relaxation the Na atoms in the subsurface layer move upwards by nearly 2 Å from their ideal positions. Hence the equilibrium surface structure is actually $Na_{1/3}|O_3|Ir_2|O_3|\cdots$, as shown in Fig. 2(b). This very large relaxation is confirmed experimentally by the excellent agreement between experimental and simulated empty-state images. The filled-state images are also in very good agreement. Interestingly, they do not show any contrast reversal. Instead, the topography in filled-state images actually arises from oxygen orbitals that are neighbors of surface Na atoms, whereas the empty-state images are dominated by the unoccupied Na orbitals themselves. Both the periodicity and topography of the empty-states images are entirely determined by empty Na states, which can only be the case if the Na atoms have relaxed completely out of the subsurface Ir layer. Such a relaxation is an essential aspect of the surface science of this material class. Furthermore, it is possible that the reconstruction due to Na diffusion is only facilitated by temperature, suggesting a study of the surface phase diagram.

Our proposal, based on the comparison of STM data to simulated images, is rather unexpected and needs to be verified by other experiments. However, the combination of STM and DFT is a good starting point and the developed structural models and bias-dependent information for filled and empty states as it is provided here is a test of the predicted structure.

We next performed a spectral analysis of the two surface terminations using STS to investigate their electronic structure. Figure 3(a) shows the differential conductivity dI/dV of both surface structures. The gaps are estimated to $E_g \approx 1.2$ eV on the 1×1 surface and $E_g \approx 0.6$ eV on the $(\sqrt{3}\times\sqrt{3})R30^\circ$ surface [13]. One might be tempted to compare these numbers, especially the less strongly reconstructed 1×1, with the optical and angle-resolved photoemission spectroscopy (ARPES) gap of 340 meV reported in Ref. [14]. However, this discrepancy must be taken with a grain of salt because optical absorption is a bulk probe and it is only natural that the surface gap, after reconstruction and relaxation, is very different—including the effects of the less well-screened Hubbard U at the surface.

Regarding ARPES, which is indeed a surface probe, in order to access the excitation gap, in Ref. [14] the surface of Na_2IrO_3 was coated with K, to shift the chemical potential into the upper Hubbard band. As we observe a 600 meV difference between different Na_2IrO_3 surfaces, coating with K should have a serious effect on the gap. Moreover, the surface in [14] probably also consisted of an ensemble of two reconstructions as found here. Hence to directly compare the surface gap obtained from STS and K-doped ARPES, all these issues need to be considered.

Comin *et al.* decomposed angle-integrated photoemission spectra [14] between -2 and 0 eV into four Gaussians, consistent with the band structure calculation [7]. Our experimental DOS, which we estimate in Fig. 3(b) by averaging

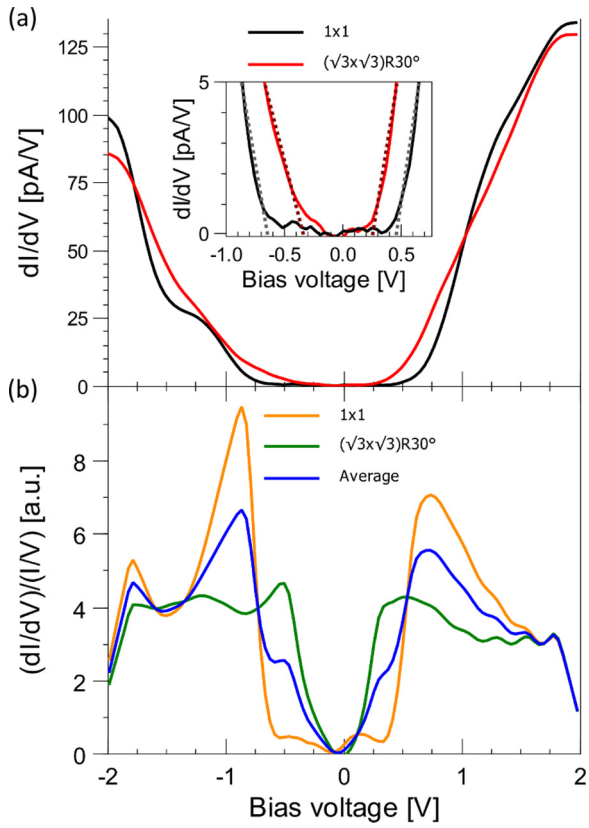

FIG. 3. (Color online) (a) Differential conductivity spectra of the 1×1 and $(\sqrt{3}\times\sqrt{3})R30^\circ$ surface. The inset shows a zoom into the onset region of conduction and valence bands. The gap is estimated by linear extrapolation of the band edges to zero conductance, indicated as dashed lines [13]: For the 1×1 surface we observe the gap to be $E_g \approx 1.2$ eV, while the $(\sqrt{3}\times\sqrt{3})R30^\circ$ surface shows a smaller gap of $E_g \approx 0.6$ eV. (b) Normalized differential conductivity graphs of the two surfaces and their average. Spectral features are visible at $V_{\text{bias}} \simeq \pm1$ V. The averaged spectrum, assuming equal surface coverages, allows a comparison to ARPES and optical conductivity measurements. Note: The signal inside the gap is below the setup resolution limit and apparent features are computational noise [13].

the normalized conductivity $(dI/dV)/(I/V)$ over the two surfaces, is largely consistent with this observation. Note that the higher-bias DOS is somewhat overestimated in the measurements, probably due to incomplete cancellation of the tunneling matrix elements and the band edges are distorted due to the calculation process. It is worth noting that in Ref. [14], as well as in our experiment, the centers of the occupied bands are shifted by 0.1–0.3 eV to lower energies, which would also increase the minimal gap.

Nevertheless, the decomposition of the angle-integrated photoemission spectra between -2 and 0 eV corresponding to the four bands described above and the consistence with theory might be fortuitous. Indeed, accurate modeling of the ARPES spectra may require including spectral features of both surface reconstructions (with similar weights), as suggested by our structural analysis. Overall, the significantly larger gap found in STS remains an open issue.

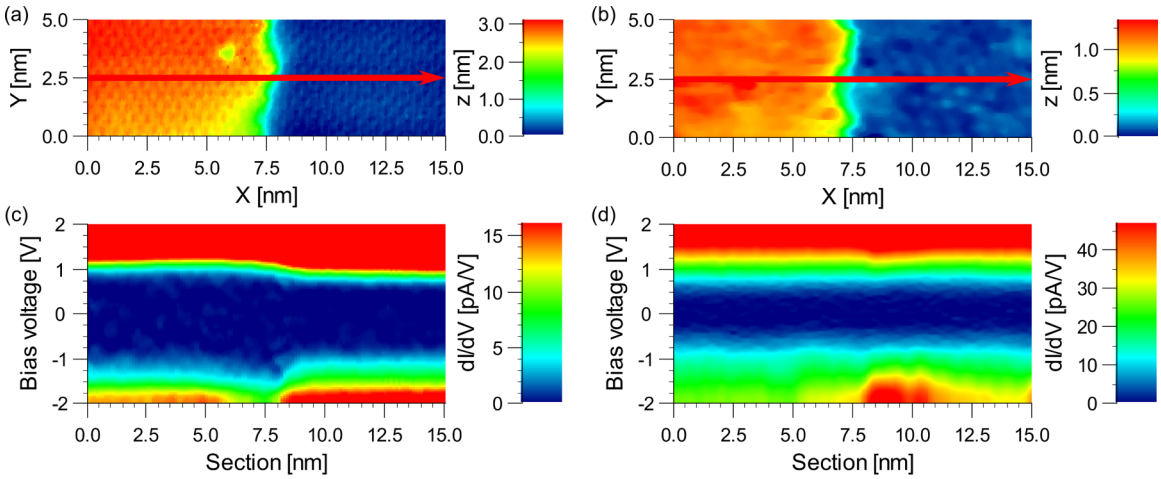

FIG. 4. (Color online) (a) STM topography of a surface step between two equivalent 1×1 surfaces. The step height is $h \approx 26.5\,\text{Å}$, corresponding to five unit cells of Na_2IrO_3. (b) Topography of a surface step separating two equivalent $(\sqrt{3} \times \sqrt{3})R30^\circ$ surfaces. The step height is $h \approx 10.6\,\text{Å}$, corresponding to two unit cells. (c) Differential conductivity spectra along the red line in (a). We observe a smooth transition and a slightly larger gap on the upper terrace. The full gap is evident throughout the line scan. (d) Differential conductivity spectra along the red line in (b). The gap is maintained across the step edge with only small fluctuations within the valence and conduction bands.

Considering the STS spectra, tip-induced band bending might be a possible candidate to explain an apparent increase of the gap. Our topographic data show that the surfaces exhibit atomic scale defects, leading to the expectation of Fermi level pinning inside the gap, similar to results on semiconductor surfaces [15]. This scenario implies that STS does indeed reflect a significantly larger surface gap.

Finally, we address the issue of QSH behavior. Reference [2] predicted that Na_2IrO_3 is a QSH insulator and therefore that the gap must briefly close as a step is traversed. However, as we have established, the surface of Na_2IrO_3 is rather different from the bulk. Even if the model of Ref. [2] correctly captures the relevant features of the bulk band structure, it may be not applicable to the actual surfaces that are realized in nature. With this caveat in mind, we have monitored the tunneling gap as the tip traverses a step (Fig. 4). The observed step heights are in agreement with the crystal structure [16] and correspond to the height of five unit cells (26.5 Å) and two unit cells (10.6 Å), respectively. Figures 4(c) and 4(d) show spatially resolved STS spectra taken along the red lines in Figs. 4(a) and 4(b). Upon traversing a step separating two 1×1 surfaces, a smooth transition can be observed with no sign of gap closure anywhere. The step separating two $(\sqrt{3} \times \sqrt{3})R30^\circ$ regions likewise shows a constant gap with no sign of closure. We conclude that neither of the two possible terminations of Na_2IrO_3 shows any evidence of the QSH effect.

This work was supported by the DFG priority program 1666 and the Helmholtz Virtual Institute 521, and in part by the U.S. Office of Naval Research through the Naval Research Laboratory's Basic Research Program.

[1] B. J. Kim, H. Ohsumi, T. Komesu, S. Sakai, T. Morita, H. Takagi, and T. Arima, Science **323**, 1329 (2009).
[2] A. Shitade, H. Katsura, J. Kunes, X.-L. Qi, S.-C. Zhang, and N. Nagaosa, Phys. Rev. Lett. **102**, 256403 (2009).
[3] D. Pesin and L. Balents, Nat. Phys. **6**, 376 (2010).
[4] J. Chaloupka, G. Jackeli, and G. Khaliullin, Phys. Rev. Lett. **105**, 027204 (2010).
[5] H.-C. Jiang, Z.-C. Gu, X.-L. Qi, and S. Trebst, Phys. Rev. B **83**, 245104 (2011).
[6] I. I. Mazin, H. O. Jeschke, K. Foyevtsova, R. Valentí, and D. I. Khomskii, Phys. Rev. Lett. **109**, 197201 (2012).
[7] K. Foyevtsova, H. O. Jeschke, I. I. Mazin, D. I. Khomskii, and R. Valentí, Phys. Rev. B **88**, 035107 (2013).
[8] Y. Singh and P. Gegenwart, Phys. Rev. B **82**, 064412 (2010).
[9] G. Kresse and J. Hafner, Phys. Rev. B **47**, 558 (1993).
[10] G. Kresse and J. Furthmüller, Phys. Rev. B **54**, 11169 (1996).
[11] J. Tersoff and D. R. Hamann, Phys. Rev. B **31**, 805 (1985).
[12] Although it is possible to construct surface models having $(\sqrt{3} \times \sqrt{3})R30^\circ$ periodicity without fully depleting the topmost Na layer, these are strongly contradicted by the observed STM topography.
[13] R. M. Feenstra, Phys. Rev. B **50**, 4561 (1994).
[14] R. Comin, G. Levy, B. Ludbrook, Z.-H. Zhu, C. N. Veenstra, J. A. Rosen, Y. Singh, P. Gegenwart, D. Stricker, J. N. Hancock, D. van der Marel, I. S. Elfimov, and A. Damascelli, Phys. Rev. Lett. **109**, 266406 (2012).
[15] R. M. Feenstra and P. Mårtensson, Phys. Rev. Lett. **61**, 447 (1988).
[16] S. K. Choi, R. Coldea, A. N. Kolmogorov, T. Lancaster, I. I. Mazin, S. J. Blundell, P. G. Radaelli, Y. Singh, P. Gegenwart, K. R. Choi, S.-W. Cheong, P. J. Baker, C. Stock, and J. Taylor, Phys. Rev. Lett. **108**, 127204 (2012).